Available online at www.sciencedirect.com
SCIENCE DIRECT®

Catalysis Today 96 (2004) 31–41

CATALYSIS TODAY

www.elsevier.com/locate/cattod

In situ FTIR studies of the mechanism of NO_x storage and reduction on $Pt/Ba/Al_2O_3$ catalysts

Yu Su, Michael D. Amiridis*

Department of Chemical Engineering, University of South Carolina, Columbia, SC 29208, USA

Abstract

The mechanism of NO_x adsorption and reaction on a typical 1 wt.% Pt/20 wt.% BaO/Al_2O_3 NO_x storage reduction (NSR) catalyst was studied by the use of in situ Fourier Transform InfraRed (FTIR) spectroscopy. Parallel studies were also conducted with the individual components of the NSR system (i.e., 1 wt.% Pt/Al_2O_3 and 20 wt.% BaO/Al_2O_3) in an effort to identify the role and importance of each component in the NSR process. Finally, the role of SO_2 was also investigated, since it has been reported that it represents a poison for the NSR process. The results indicate that at 350 °C NO_x is stored on the NSR catalyst primarily in the form of barium nitrite and nitrate species. In the presence of Pt a conversion of the surface barium nitrite to bulk barium nitrate is taking place during the storage phase. This step is accelerated in the presence of gas phase oxygen and at elevated temperatures. Both barium nitrite and nitrate species are reduced in the presence of propylene, although at different rates. These reactions are catalyzed by Pt and do not proceed at any significant rate over the BaO/Al_2O_3 sample. Finally, the formation of surface and bulk barium sulfates was observed when SO_2 was introduced as a component of the NO-containing gas phase mixture. These species are stable on the catalyst surface under the reduction conditions studied and inhibit the NO_x storage process.

Keywords: NSR catalysts; NO_x storage; NO_x reduction; SO_2

1. Introduction

Automobile manufacturers have demonstrated that the use of “lean-burn” engines (i.e., engines which operate under excess oxygen conditions) can result in a substantial decrease of fuel consumption, and therefore, CO_2 emissions [1]. However, under such conditions, the three-way catalysts used to treat the exhaust of conventional engines cannot reduce the NO_x concentrations down to the levels required by federal and local regulations. Over the last decade a substantial research effort has been devoted to developing new catalytic systems capable of meeting current NO_x emission standards for “lean-burn” engines. Much of this effort has focused on the selective catalytic reduction of NO by hydrocarbons (HC-SCR). Nevertheless, as reviews of this field point out, current HC-SCR catalysts do not have the required activity and/or stability to meet these standards [2,3].

As an alternative to a single catalytic step reduction process, industrial workers in this field have developed a stepwise approach involving the storage and reduction of NO_x in two distinct steps conducted under different conditions [4–6]. This approach, utilizes materials—termed NO_x storage reduction (NSR) catalysts—that are capable of storing nitrogen oxides under lean conditions, and subsequently, releasing and reducing them under a short pulse of fuel rich conditions. In the most commonly used NSR system, the storage function is achieved on BaO, while the catalytic function is provided by Pt. An alumina support is also used for dispersion purposes, while additional components—such as Rh and TiO_2—may also be included in different formulations to satisfy stability and regeneration requirements (especially in the presence of SO_2). Such an NSR system has been successfully commercialized in Japan [6,7].

Several publications have appeared in the open literature recently, indicating that substantial research activity is currently focusing on different aspects of NSR catalysts. The majority of these reports are examining different performance characteristics of the NSR catalytic systems, and in particular, the effect of the operating conditions, such as the

---

* Corresponding author.
E-mail address: amiridis@engr.sc.edu (M.D. Amiridis).

0920-5861/$ – see front matter © 2004 Elsevier B.V. All rights reserved.
doi:10.1016/j.cattod.2004.05.005

composition and temperature of the exhaust and the length of the lean/rich cycles [6,8–13]. Less of an attempt has been made so far to develop a comprehensive understanding of the fundamental surface chemistry involved in the storage and/or reduction steps. Work in this area has primarily utilized in situ FTIR spectroscopy and investigated the effect of individual components of the exhaust stream (i.e., the interaction of nitrogen oxides or hydrocarbons with the catalyst surface) or individual cycles of the NSR process (i.e., adsorption/reaction taking place under lean conditions) [14–18] Additional FTIR studies have also focused on the interaction of SO_2 with NSR catalysts, since these systems are known to deactivate in the presence of SO_2 in the exhaust due to the formation of stable alkaline earth metal sulfates [7,19–21].

The work described in this manuscript represents our first step of a systematic fundamental investigation of the mechanisms that govern the reactivity and stability of NSR catalysts. Materials were prepared containing either one or both active components of the NSR system (i.e., Pt and BaO) on an alumina support. The interaction of these materials with the gases involved in the NO_x reduction process (i.e., NO, O_2 and hydrocarbons), as well as with SO_2 were investigated at room temperature, as well as 350 °C via FTIR spectroscopy. In addition, some cyclic studies were conducted involving switching from a lean to a rich environment, in an attempt to identify the active species involved not only in NO_x storage, but also in the reduction step.

2. Experimental

2.1. Catalyst preparation

All catalysts used in this study (i.e., 1 wt.% Pt/Al_2O_3, 20 wt.% BaO/Al_2O_3 and 1 wt.% Pt/20 wt.% BaO/Al_2O_3) were prepared through an incipient wetness impregnation process on a γ-Al_2O_3 support (Vista Chemical Co.). Prior to the impregnation, the support was calcined overnight at 500 °C in air. $H_2PtCl_6{\cdot}6H_2O$ (Aldrich Chemical Co.) and $Ba(CH_3COO)_2$ (Aldrich Chemical Co.) were used as the precursors for Pt and BaO, respectively. Following impregnation, the samples were washed, dried at 120 °C for 2 h and then calcined in air for 5 h at 500 °C. Elemental analysis (Galbraith Laboratories) of the catalysts thus prepared indicates less than 23 ppm in total halogen concentration, suggesting that most of the chloride precursor was removed and it is unlikely to have affected catalytic performance. While this process results in the decomposition of the barium acetate precursor, it yields a mixture of barium carbonate and barium oxide (as indicated by subsequent XRD and FTIR results observed in this study, as well as in others). Therefore, it should be pointed out that although throughout this manuscript we refer to the catalyst loading and composition in terms of BaO, this reference should not be interpreted literally to represent the chemical nature of the Ba being present in the fresh catalyst.

Table 1
BET and chemisorption data

	1% Pt/Al_2O_3	1% Pt/20% BaO/Al_2O_3	20% BaO/Al_2O_3
Surface area (m^2/g)	147	133	137
Pt dispersion (%)	46	38	NA

2.2. Catalyst characterization

Surface areas of the different samples used in this study were determined through BET measurements with an Autosorb-1 gas sorption system (Quantachrome Corporation) at 77 K. The results of these measurements are summarized in Table 1. Furthermore, for the two platinum-containing samples, platinum dispersions were determined through hydrogen chemisorption measurements conducted on the same gas sorption system. These results are also summarized in Table 1. Finally, the samples were also analyzed through X-ray diffraction measurements on a Rigaku D-max B single axis diffractometer with a Cu Kα ($\lambda = 0.1543$ nm) radiation source. The XRD patterns obtained indicate that Ba exists primarily in the form of barium carbonate in the as-prepared samples. It is still possible however, that other amorphous or highly dispersed phases containing Ba may be present in these samples.

2.3. FTIR spectroscopy studies

FTIR spectra were collected with a Nicolet 740 Fourier transform infrared (FTIR) spectrometer operating in the transmission mode, with a resolution of 2 cm^{-1}. Spectra of the as-prepared surfaces in flowing He were collected separately at the temperature of the measurements prior to any treatment and were used as references. A stainless steel IR cell with NaCl windows cooled by flowing water and a 10 cm path length was used for these experiments. A heating element wrapped around the cell allowed collection of in situ spectra at 350 °C. The temperature in the cell was monitored through a thermocouple located in close proximity to the catalyst sample.

Catalyst samples were prepared as self-supported wafers, 12 mm in diameter and with a “thickness” of approximately 10 mg/cm^2. KBr was added at the ratio of 3:1 for the preparation of the pellets (spectra collected with pure samples indicated that there was no effect by the KBr presence). Prior to each experiment the samples were pretreated at 400 °C in a flowing 5% O_2 in He mixture for 1 h.

Certified analyzed mixtures of 1.00% NO in He, 0.975% C_3H_6 in He, 10.00% O_2 in He, 1.0003% SO_2 in He and a 99.9999% He carrier gas (National Specialty Gases) were used to prepare the different gas mixtures. Typical concentrations used were 1000 ppm of NO, 1000 ppm C_3H_6, 5% O_2 and 1000 ppm SO_2. Gases were mixed at the appropriate amounts by the use of a system of needle valves and flow meters and preheated prior to the introduction to their cell.

The total volumetric flow rate of the gas mixtures over the catalyst samples was held constant at 100 cm^3/min.

3. Results and discussion

3.1. NO adsorption

3.1.1. Pt/Al_2O_3

The spectrum of a Pt/Al_2O_3 sample exposed to 1000 ppm NO in He mixture at room temperature for 5 min is shown in Fig. 1 (spectrum a). This spectrum contains several peaks in the range of 1200–1700 cm^{-1}. According to previous literature reports, all of these peaks can be assigned to different types of surface nitrate and nitrite species associated with the alumina support. In particular, the peaks at 1230 and 1477 cm^{-1} can be assigned to bridged bidentate and linear nitrite species respectively, while the peaks at 1340, 1556 and 1630 cm^{-1} can be assigned to monodentate, bidentate, and bridging nitrate species [14,17]. The assignments of the various peaks observed in this study to adsorbed N_xO_y and sulfate species are summarized in Table 2. The oxygen needed for the formation of these species from NO is probably present on the Pt surface as a result of the pre-oxidation treatment. When 5% O_2 was added to the gas phase NO/He mixture (Fig. 1, spectrum b), the same peaks were observed in the spectrum, although the intensity of the nitrate peaks was slightly higher, consistent with a higher degree of oxidation of NO in this case. The effect was relatively small, probably because of the oxidation pretreatment conditions used.

Table 2
IR assignments for adsorbed N_xO_y and sulfate species

	Wave numbers (cm^{-1})	Reference
N_xO_y species on Al_2O_3		
Bridging nitrite	1230, 1340	[14,17]
Linear nitrite	1477	[14,17]
Chelating bidentate nitrate	1552	[14,17]
Bidentate nitrate	1556	[14,17]
Bridging nitrate	1592, 1630	[14,17]
N_xO_y species on BaO		
Bridging nitrite	1237	[14,17]
Monodentate nitrate	1337	[14,17]
Hyponitrite	1386	[14,17]
Bridging nitrate	1592, 1626	[14,17]
Sulfate species on Al_2O_3		
S=O vibration	1360	[21,22]
S–O vibration	1038	[21,22]
Sulfate species on BaO		
S=O vibration	1127	[21,23]
S–O vibration	1087	[21,23]

When the adsorption of NO was carried out at 350 °C (Fig. 1, spectrum c) a substantial decrease was observed in the intensity of all nitrate/nitrite peaks, consistent with the relatively low thermal stability of these species on alumina. Most notable is the complete elimination of the 1477 and

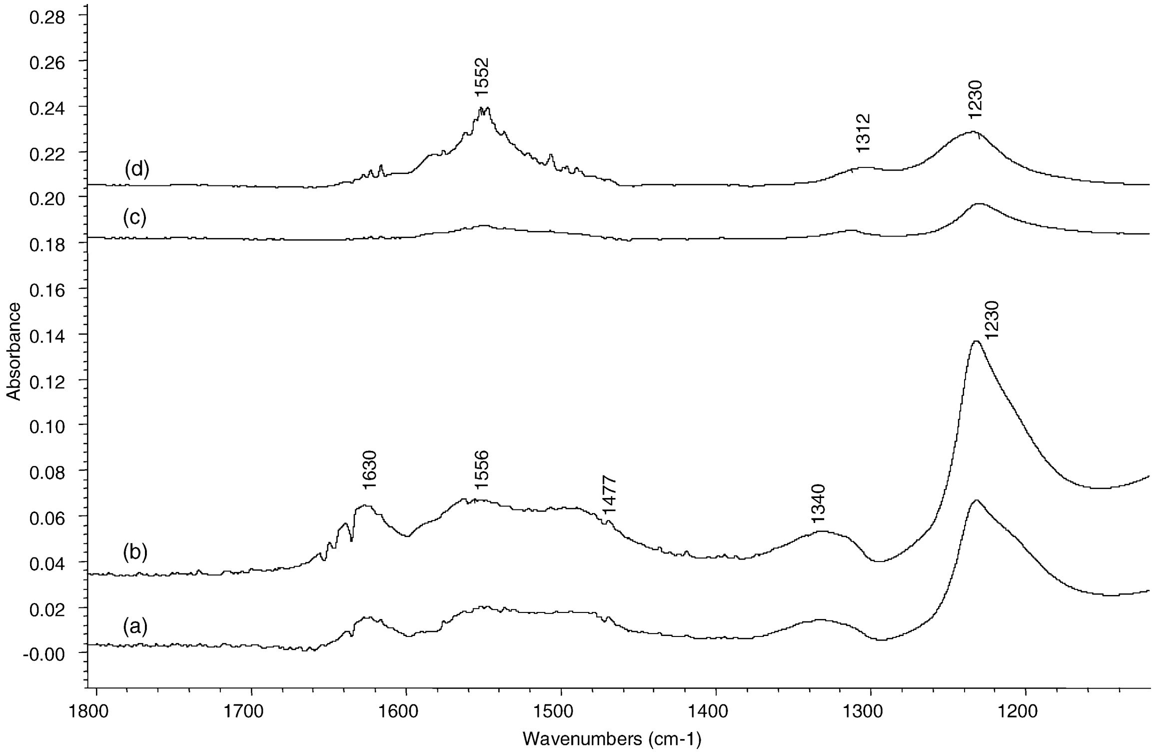

Fig. 1. Spectra collected following exposure of a pre-oxidized Pt/Al_2O_3 catalyst to: (a) 1000 ppm NO in He at 25 °C for 5 min; (b) 1000 ppm NO, 5% O_2 in He at 25 °C for 5 min; (c) 1000 ppm NO in He at 350 °C for 5 min; (d) 1000 ppm NO, 5% O_2 in He at 350 °C for 5 min.

1630 cm^{-1} peaks, corresponding to the linear nitrite and bridging nitrate species. Furthermore, the peak at 1340 cm^{-1} shifts to 1312 cm^{-1}, while the peak at 1552 cm^{-1} becomes the most pronounced nitrate feature and exhibits several shoulders. These changes indicate a modification in the structure of the nitrate species with temperature, and suggest that chelating bidentate nitrate structures (with the characteristic peak at 1552 cm^{-1}) become most abundant at elevated temperatures. Similar results have also been reported by Sedlmair et al. [17] and Fanson et al. [18]. The presence of 5% O_2 in the gas phase results in an increase in the intensity of the nitrate peaks (Fig. 1, spectrum d). The effect of oxygen is more pronounced in this case than it was at room temperature, probably due to the lower amounts of surface oxygen retained at 350 °C as a result of the catalyst pretreatment.

3.1.2. *BaO/Al$_2$O$_3$*

The spectrum of a BaO/Al_2O_3 sample exposed to a 1000 ppm NO in He mixture at room temperature for 5 min is shown in Fig. 2 (spectrum a). The spectrum contains three major peaks at 1237, 1386 and 1626 cm^{-1}, which can be assigned to surface bidentate nitrite, hyponitrite and bridging nitrate species, respectively [14,17]. The formation of bidentate nitrite and bridging nitrate species was also observed with the Pt/Al_2O_3 sample, with very similar positions of the corresponding peaks in the spectrum. In contrast, the hyponitrite is a new species, which is presumably formed exclusively on barium.

When 5% O_2 was added to the gas phase NO/He mixture, several changes were observed in the corresponding spectrum (Fig. 2, spectrum b). In particular, the 1386 cm^{-1} peak was replaced by a new feature at 1337 cm^{-1}, indicating the oxidation of the hyponitrite species on barium and the formation of a monodentate nitrate species. In addition, the nitrite peak at 1237 cm^{-1} grew substantially in intensity indicating a much higher concentration of this species on the BaO/Al_2O_3 sample, as compared to the Pt/Al_2O_3 sample.

When the adsorption of NO was carried at 350 °C (Fig. 2, spectrum c) the nitrite peak at 1237 cm^{-1} was the only significant feature remaining in the spectrum, indicating a relatively lower thermal stability for all other nitrate/nitrite species. Furthermore, a very broad and weak negative peak—which can be assigned to barium carbonate [15,17]—appears in spectrum 2c centered at approximately 1458 cm^{-1}, suggesting that the decomposition of the remaining barium carbonate in the sample can be initiated in the presence of nitrogen oxides at this temperature. Both the formation of the nitrite species and the decomposition of the barium carbonate are facilitated by the presence of 5% oxygen in the gas phase (Fig. 2, spectrum d).

3.1.3. *Pt/BaO/Al$_2$O$_3$*

Spectra of a $Pt/BaO/Al_2O_3$ sample exposed to a 1000 ppm NO in He mixture at room temperature for 5 min in the presence and absence of 5% O_2 in the gas phase are shown in Fig. 3 (spectra a and b). When compared to the corresponding spectra obtained with the individual components of the material (i.e., Pt/Al_2O_3 and BaO/Al_2O_3) shown in Figs. 1 and 2, it becomes apparent that there is no synergistic effect of Pt and Ba at room temperature. In fact, the spectra of the $Pt/BaO/Al_2O_3$ sample are very similar to the

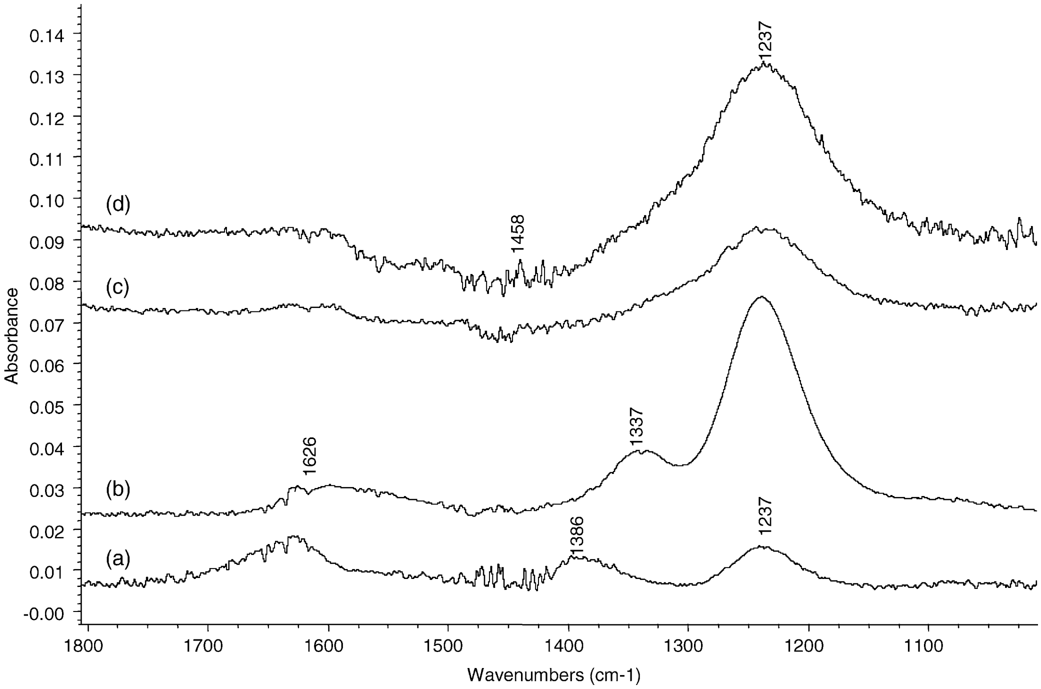

Fig. 2. Spectra collected following exposure of a pre-oxidized BaO/Al_2O_3 catalyst to: (a) 1000 ppm NO in He at 25 °C for 5 min; (b) 1000 ppm NO, 5% O_2 in He at 25 °C for 5 min; (c) 1000 ppm NO in He at 350 °C for 5 min; (d) 1000 ppm NO, 5% O_2 in He at 350 °C for 5 min.

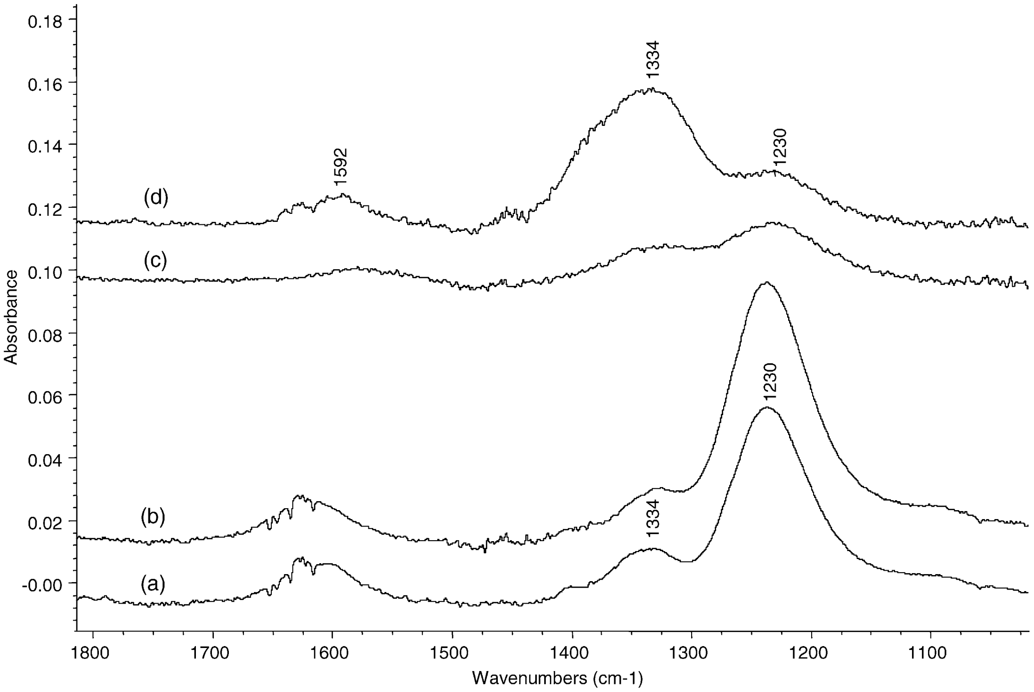

Fig. 3. Spectra collected following exposure of a pre-oxidized 1%Pt/BaO/Al_2O_3 catalyst to: (a) 1000 ppm NO in He at 25 °C for 5 min; (b) 1000 ppm NO, 5% O_2 in He at 25 °C for 5 min; (c) 1000 ppm NO in He at 350 °C for 5 min; (d) 1000 ppm NO, 5% O_2 in He at 350 °C for 5 min.

spectra obtained with the BaO/Al_2O_3 sample (Fig. 2). The only difference is an increased intensity of the nitrite peak at 1230 cm^{-1} in the absence of O_2.

In contrast, a synergistic effect between Pt and Ba becomes apparent when a comparison is attempted between spectra of the Pt/BaO/Al_2O_3 system (Fig. 3, spectra c and d) and the corresponding spectra of the Pt/Al_2O_3 and BaO/Al_2O_3 components (Figs. 1 and 2, spectra c and d) obtained at 350 °C. The main nitrogen-containing species observed in this case are bidentate nitrites (1230 cm^{-1}), monodentate nitrates (1334 cm^{-1}) and bidentate nitrates (main peak at 1592 cm^{-1}). The results of the studies conducted with the individual components, suggest that the nitrite and monodentate nitrate species are associated with the Ba component, while the bidentate nitrate species is associated with Al (formed however, on Pt). Furthermore, results of desorption studies suggest that the bidentate nitrate species is not strongly held on the Al component and is easily removed within seconds following the removal of NO from the gas phase. In contrast—as discussed below—the nitrite and monodentate nitrate species on the Ba component exhibit a much higher stability and remain on the surface following treatments at 350 °C with He and a 5% O_2 in He mixture.

Spectra collected at different time intervals during the exposure of the Pt/BaO/Al_2O_3 sample to the NO/He and NO/O_2/He mixtures are shown in Fig. 4. These spectra indicate a different behavior for the nitrite and nitrate species associated with the Ba component. In particular, while the nitrite peak appears immediately following exposure to the gas phase mixtures containing NO and remains approximately constant in intensity thereafter, the nitrate peak develops slowly over time and continues to increase in intensity throughout the experiments shown. After 10 min on stream it reaches the same intensity as the nitrite peak in the absence of oxygen, while it is clearly the dominant feature of the spectrum in the presence of oxygen. These results indicate that the process of conversion of nitrite to nitrate species is accelerated in the presence of oxygen (an anticipated result, since an oxidation step is involved). Furthermore, this process appears to be catalyzed by Pt, since no such behavior was observed with the BaO/Al_2O_3 component.

Studies of longer duration have shown that a saturation level is finally reached after longer time periods (on the order of 60 min in the presence and 90 min in the absence of oxygen). Furthermore, upon removal of NO from the gas phase and flushing on the nitrate/nitrite containing surface (Fig. 5, spectrum a) with a 5% O_2 in He mixture, the remaining nitrite species is converted to the nitrate species as indicated by the disappearance of the 1230 cm^{-1} peak and the slight increase in intensity of the 1334 cm^{-1} peak (Fig. 5, spectrum b). The involvement of barium nitrite and nitrate species in the mechanism of NO_x storage on Ba has also been discussed by other groups. Our results are in general agreement with those of Lietti et al. [11] and Huang et al. [16], who also suggest that NO is primarily stored in the form of a nitrate species and that a surface nitrite species is the precursor to the barium nitrate.

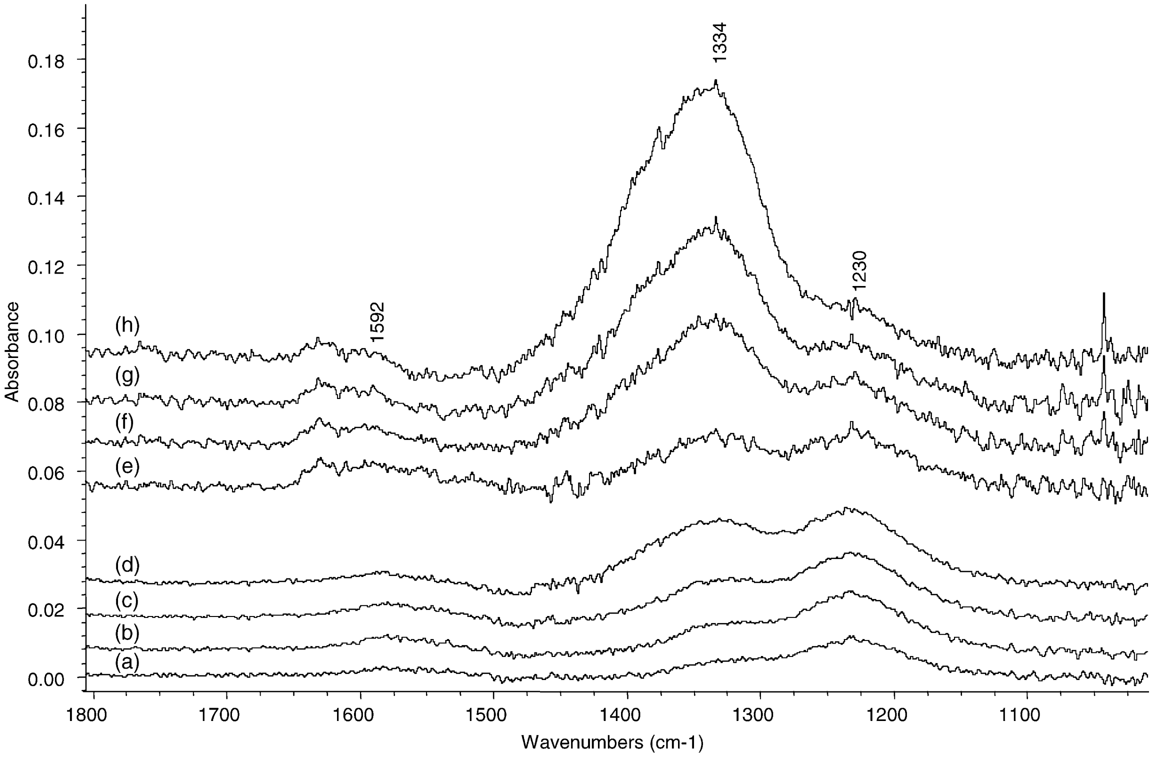

Fig. 4. Spectra collected at 350 °C following exposure of a pre-oxidized Pt/BaO/Al_2O_3 catalyst to: 1000 ppm NO in He for (a) 1 min, (b) 3 min, (c) 5 min, (d) 10 min; 1000 ppm NO, 5% O_2 in He for (e) 1 min, (f) 3 min, (g) 5 min, (h) 10 min.

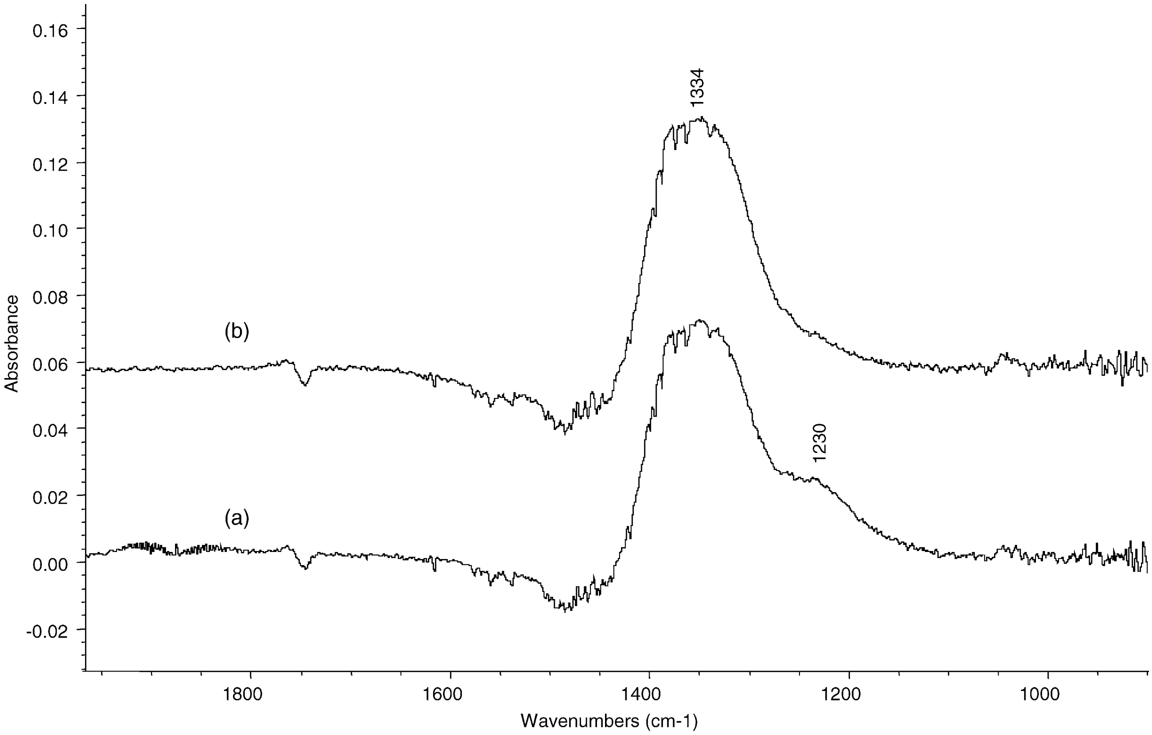

Fig. 5. Spectra collected at 350 °C following exposure of a pre-oxidized Pt/BaO/Al_2O_3 catalyst to: 1000 ppm NO in He for (a) 90 min, flush of (a) with 5% O_2 in He for (b) 10 min.

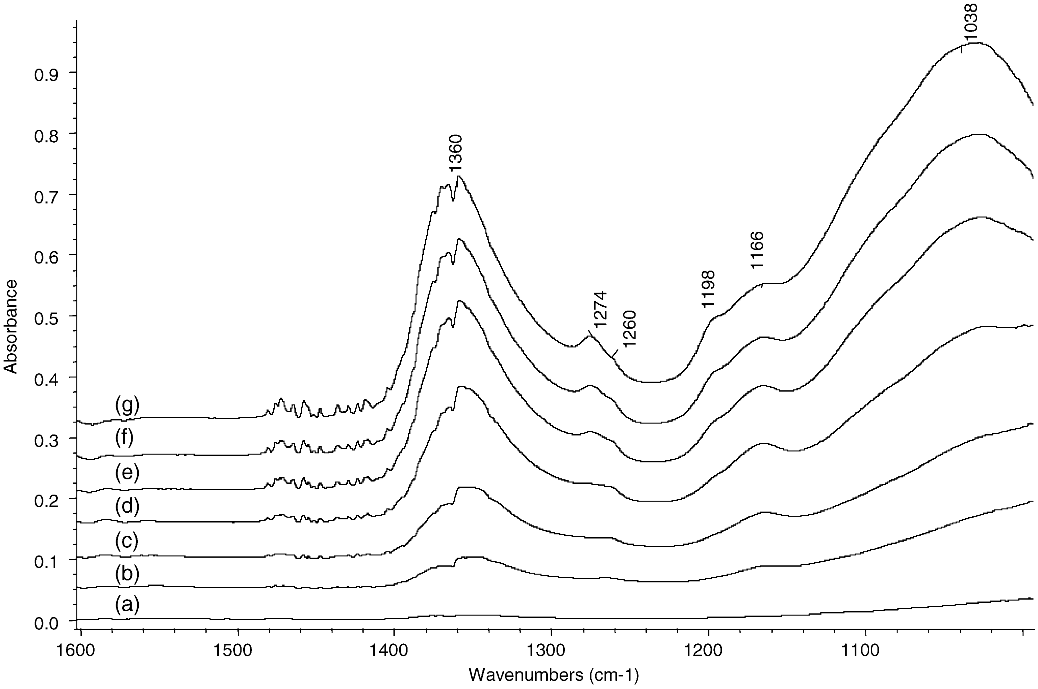

Fig. 6. Spectra collected at 350 °C following exposure of a pre-oxidized Pt/Al_2O_3 catalyst to 1000 ppm SO_2 in He for (a) 1 min, (b) 3 min, (c) 5 min, (d) 10 min, (e) 20 min, (f) 30 min, (g) 45 min.

3.2. SO_2 adsorption

3.2.1. Pt/Al_2O_3

Spectra of a Pt/Al_2O_3 sample collected at different times on stream during exposure at 350 °C to a 1000 ppm SO_2, 5% O_2 in He mixture are shown in Fig. 6. The main features of these spectra are two broad peaks centered at approximately 1360 and 1038 cm^{-1}, previously assigned by Sedlmair et al. [21,22] to the S=O and S–O vibrations respectively, of a tri-coordinated sulfate species on the alumina support. These peaks continued to grow slowly in intensity during the 45 min run, indicating a slow accumulation of the corresponding surface species. Two additional weaker peaks were also observed from the early stages of the adsorption at 1166 and 1260 cm^{-1}. These peaks have been assigned by Mahzoul et al. [19] to bulk sulfate species on alumina. The intensity of these two peaks went through a maximum with time on stream and eventually decreased after 20 min. At approximately the same time two new peaks appeared at 1198 and 1274 cm^{-1}, which can be assigned to the same S–O and S=O vibrations of bulk aluminum sulfate. These results are consistent with those of Sedlmair et al. and indicate the slow formation of bulk aluminum sulfate through a surface sulfate precursor.

3.2.2. BaO/Al_2O_3

Spectra of a BaO/Al_2O_3 sample collected at different times on stream during exposure at 350 °C to a 1000 ppm SO_2, 5% O_2 in He mixture are shown in Fig. 7. Three strong broad peaks are present in these spectra at 1185, 1127 and 1087 cm^{-1}. The peaks at 1127 and 1087 cm^{-1} can be assigned to the S–O and S=O vibrations of a surface sulfate species on barium [21,23], while the peak at 1185 cm^{-1} along with a shoulder at 1260 cm^{-1} can be assigned to bulk barium sulfate [21]. Weak shoulders are also present in the spectra of Fig. 7 at positions similar to the ones observed in the spectra of Fig. 6 (most visibly at 1360 cm^{-1}), indicating that sulfate species are also formed on the aluminum component of the BaO/Al_2O_3 sample, although the concentration of these species appears to be substantially lower than the concentration of the barium sulfate species. Finally, a negative broad peak is observed at 1458 cm^{-1}, once again indicating the decomposition of the barium carbonate precursor, and its replacement—in this case—by barium sulfate.

3.2.3. $Pt/BaO/Al_2O_3$

Spectra of a $Pt/BaO/Al_2O_3$ sample collected at different times on stream during exposure at 350 °C to a 1000 ppm SO_2, 5% O_2 in He mixture are almost identical to those of the BaO/Al_2O_3 sample shown in Fig. 7, hence, they are not included in this manuscript for brevity. These results in essence suggest that at 350 °C and in the presence of gas phase oxygen, the formation of surface sulfates through the oxidation of SO_2 is fast even in the absence of Pt. Consequently, Pt does not play a significant catalytic role in this case.

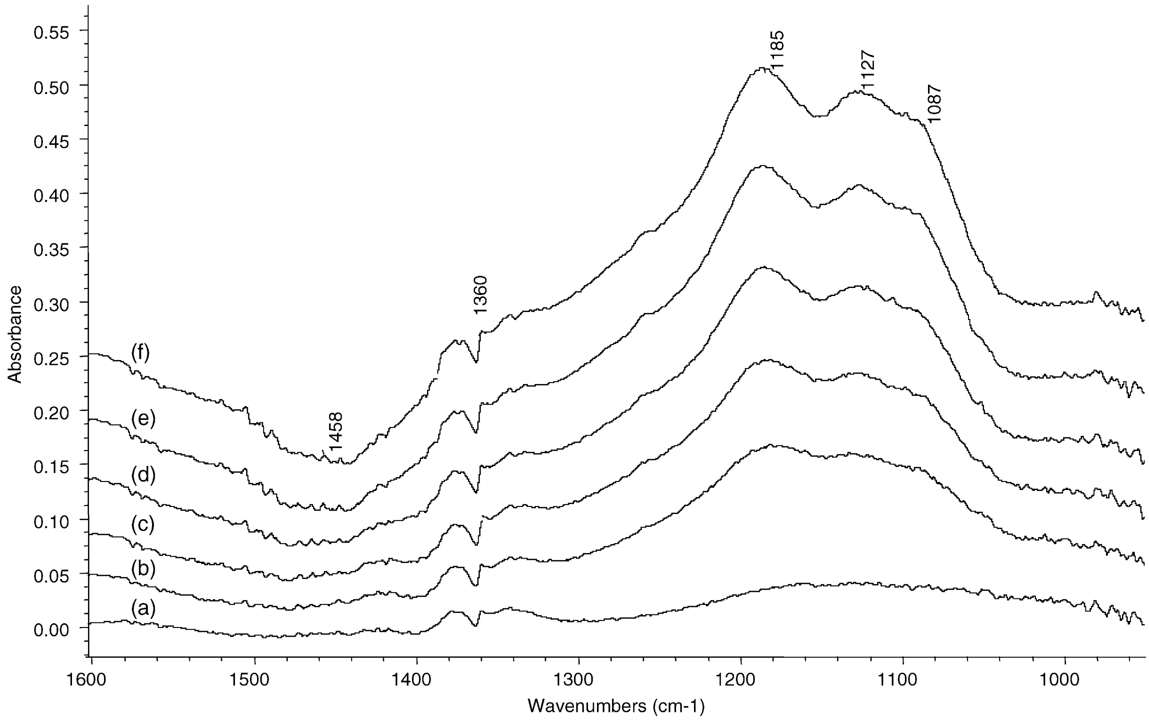

Fig. 7. Spectra collected at 350 °C following exposure of a pre-oxidized BaO/Al_2O_3 catalyst to 1000 ppm SO_2 in He for (a) 1 min, (b) 3 min, (c) 5 min, (d) 10 min, (e) 20 min, (f) 30 min.

4. Reactivity studies

4.1. $Pt/BaO/Al_2O_3$

In order to investigate the reactivity of the different nitrogen-containing species observed on the surface of the $Pt/Ba/Al_2O_3$ sample and their potential role as reactive intermediates in the NSR process, in situ FTIR studies were also conducted at 350 °C in a cyclic mode, similar to that of the actual operation of the NSR catalysts. During this type of experiments, the sample was first exposed to a short pulse of an $NO/O_2/He$ mixture, flushed for short periods of time with He and/or an O_2/He mixture to remove any weakly adsorbed species, and finally, exposed to a C_3H_6/He mixture. Spectra were collected during the different steps of this process and are shown in Fig. 8.

As discussed above, following a short exposure of the $Pt/Ba/Al_2O_3$ sample to the $NO/O_2/He$ mixture three types of nitrogen-containing species are present on the surface, namely bidentate nitrate species associated with Al and monodentate nitrate and nitrite species associated with Ba (Fig. 8, spectrum a; identical results also obtained in Fig. 4, spectrum e). The former are weakly held on the surface and are removed during the treatment with the short He and O_2/He pulses (Fig. 8, spectra b and c). As such, it is not expected that they play an important role in the NSR process. In contrast, the nitrite and nitrate species associated with Ba, can withstand these treatments and remain in significant amounts on the surface (Fig. 8, spectrum c). In fact, it appears that the interconversion of nitrite to nitrate discussed in previous paragraphs, is taking place during exposure to the O_2/He pulse.

The spectrum obtained upon exposure of the sample to the C_3H_6/He mixture (Fig. 8, spectrum d), contains two strong peaks at approximately 1345 and 1574 cm^{-1}. These peaks can be assigned respectively, to the symmetric and antisymmetric $–COO^-$ stretching vibrations of a surface acetate species formed on alumina [24]. The formation of this species is the result of the partial oxidation of propylene on Pt under the conditions employed. The 1345 cm^{-1} peak also contains a contribution from the Ba nitrate species discussed in the previous paragraph. This becomes evident from the dynamic behavior of this peak, which decreases in intensity and slightly shifts towards higher wave numbers with exposure time to the C_3H_6/He mixture (Fig. 8, spectra d–g). This decrease is not associated with a decrease in the concentration of the surface acetate species, since the intensity of the 1574 cm^{-1} peak does not follow a similar pattern and remains essentially constant. Hence, it can be attributed to the reaction of the Ba nitrate species under the reducing conditions present. The Ba nitrite species also reacts with the hydrocarbon. The reaction in this case is much faster, as indicated by the complete elimination of the corresponding 1230 cm^{-1} peak within the first minute of exposure to the C_3H_6/He mixture (Fig. 8, spectrum d).

4.2. Catalytic role of Pt component

Similar reactivity studies were also conducted with the BaO/Al_2O_3 sample in an effort to demonstrate the role of Pt

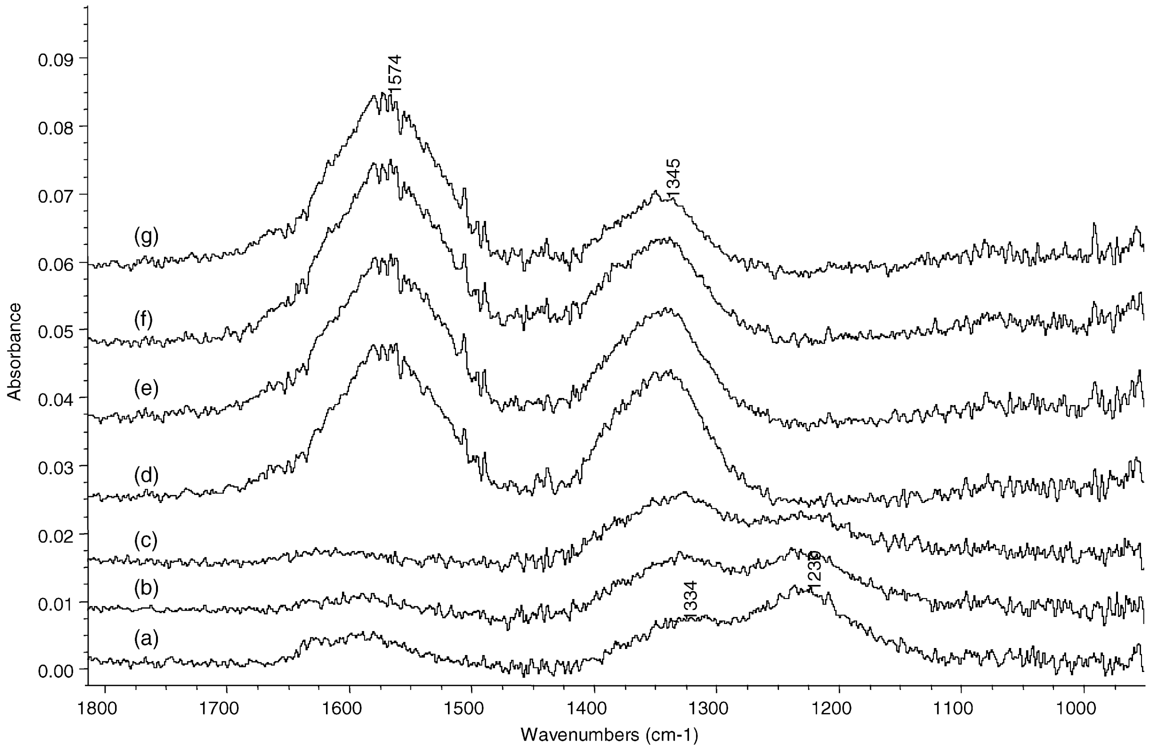

Fig. 8. Spectra collected at 350 °C during exposure of a pre-oxidized Pt/BaO/Al_2O_3 sample to: (a) 1000 ppm NO, 5% O_2 in He for 1 min; (b) flushing of (a) with He for 1 min; (c) flushing of (b) with 5% O_2 in He for 1 min; exposure of (c) to 1000 ppm C_3H_6 in He for (d) 1 min, (e) 3 min, (f) 5 min, (g) 10 min.

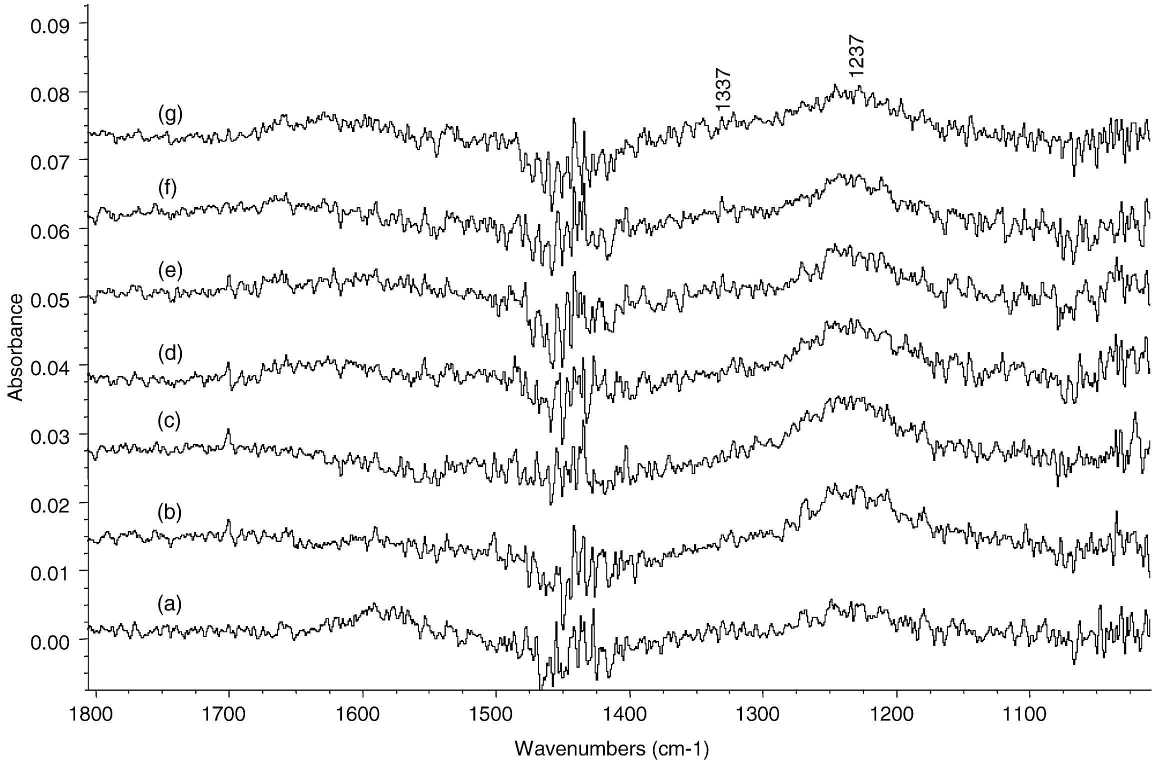

Fig. 9. Spectra collected at 350 °C during exposure of a pre-oxidized BaO/Al_2O_3 sample to: (a) 1000 ppm NO, 5% O_2 in He for 1 min; (b) flushing of (a) with He for 1 min; (c) flushing of (b) with 5% O_2 in He for 1 min; exposure of (c) to 1000 ppm C_3H_6 in He for (d) 1 min, (e) 3 min, (f) 5 min, (g) 10 min.

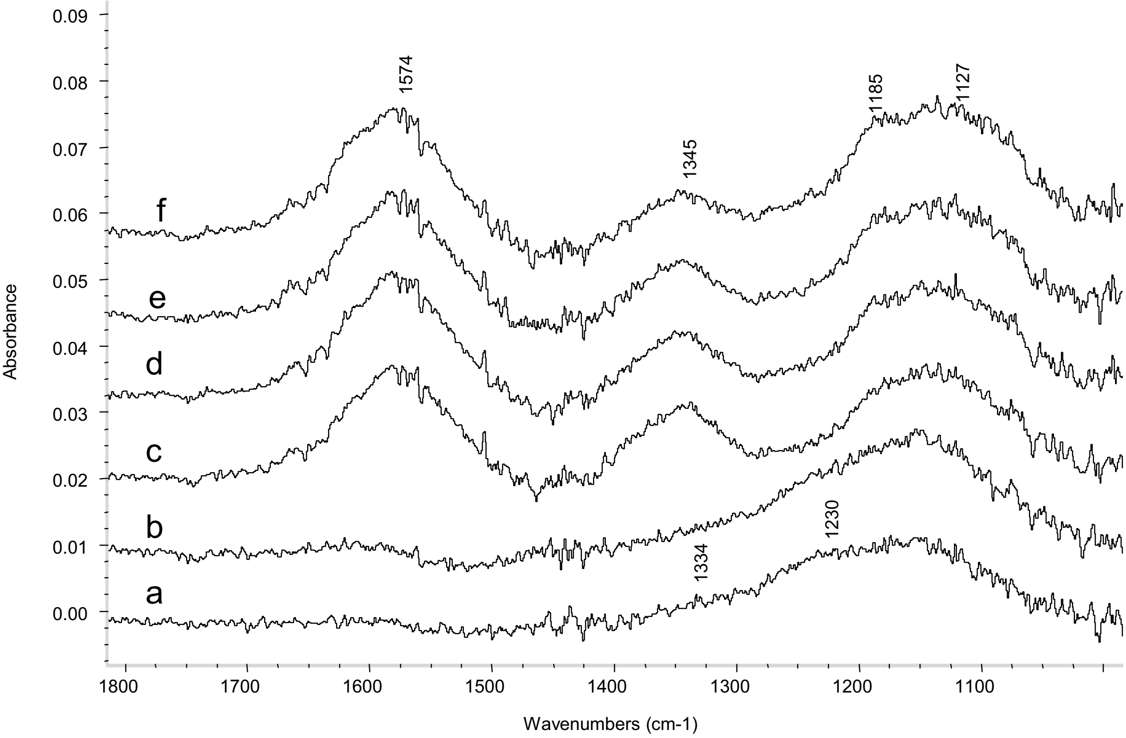

Fig. 10. Spectra collected at 350 °C during exposure of a pre-oxidized Pt/BaO/Al_2O_3 sample to: (a) 1000 ppm NO, 300 ppm SO_2, 5% O_2 in He for 2 min; (b) flushing of (a) with 5% O_2 in He for 1 min; exposure of (b) to 1000 ppm C_3H_6 in He for (c) 1 min, (d) 3 min, (e) 5 min, (f) 10 min.

in the NSR process. Spectra collected over this sample under identical conditions to the ones described in the previous section are shown in Fig. 9.

In the absence of Pt, the BaO/Al_2O_3 sample can still store nitrogen-containing species that can withstand short treatments with He and O_2/He pulses as shown in spectra a–c of Fig. 9. The amount of stored NO_x however, is substantially lower, as can be seen through a comparison with the intensity of the corresponding features in spectra a–c of Fig. 8. Furthermore, in the absence of Pt, the stored nitrogen-containing species are almost exclusively in the form of Ba nitrite, indicating that Pt is needed for the transformation of the nitrite to the more stable nitrate species. The Ba nitrite formed in this case is not reduced by the hydrocarbon when the sample is exposed to the C_3H_6/He mixture as indicated by the stable intensity of the corresponding peak at 1230 cm^{-1} (Fig. 9, spectra d–g). This result suggests that some activation of the reducing agent—and possibly the formation of a partially oxidized active intermediate—is taking place on Pt during the fuel rich phase of the NSR cycle.

4.3. *Effect of SO_2*

The effect of SO_2 on the NSR process was investigated by repeating over the Pt/BaO/Al_2O_3 sample the same set of experiments described above, but this time with an additional 300 ppm of SO_2 present during the NO_x storage phase. The spectra collected under these conditions are shown in Fig. 10. During exposure of the Pt/BaO/Al_2O_3 sample to the NO/SO_2/O_2/He mixture both surface nitrite/nitrate and sulfate species are formed on the Ba component, as indicated by the presence of various broad peaks in the 1000–1400 cm^{-1} region in spectrum a of Fig. 10 (nitrites at 1230 cm^{-1}, nitrates at 1334 cm^{-1}, and sulfates at 1127 and 1185 cm^{-1}, according to the assignments discussed previously). By comparison to the corresponding spectrum of Fig. 8 however, one can observe a much lower intensity for the nitrite and nitrate peaks, hence, demonstrating that the presence of the sulfate species inhibits the NO_x storage process, a result already observed by others in kinetic studies [25]. Furthermore, the spectra collected during the treatment with the O_2/He pulses (spectrum b of Fig. 10), as well as during the reduction phase (spectra c–f of Fig. 10), demonstrate the high stability of the sulfate species, since the intensities of the corresponding peaks remain constant during these treatments. The only difference observed was in the relative ratio of the 1185 to the 1127 cm^{-1} peak, which appears to increase slightly with time on stream. This result suggests that even in the absence of gas phase SO_2 and under reducing conditions, a transformation is taking place on the Ba component from surface to bulk sulfate at 350 °C.

5. Conclusions

An in situ FTIR investigation of the adsorption and reaction of NO has been carried out over Pt/BaO/Al_2O_3, Pt/Al_2O_3 and BaO/Al_2O_3 samples. In the 350 °C temperature range NO_x is stored on these materials primarily in the form of nitrite and nitrate species associated with barium. The formation of the later is slower and is catalyzed by Pt. As expected for an oxidation step, this process is also accelerated in the presence of gas phase oxygen and at elevated temperatures. Similar types of nitrite and nitrate species are also formed on alumina. Their concentration and stability however, are lower that those of the corresponding barium species, in agreement with the previously identified role of Ba in the NO_x storage process.

Both barium nitrite and nitrate can be fully reduced in the presence of propylene. The results suggest that a step catalyzed by Pt is involved in this process, since the reduction does not take place on the BaO/Al_2O_3 sample. The barium nitrite reacts faster than the barium nitrate. Diffusional limitations may be involved in the latter case, since the nitrate species probably contain a substantial bulk component. Nevertheless, even the reduction of the nitrate can be carried out completely, demonstrating the fully reversible nature of the NO_x storage on barium, a critical aspect for the long term application of the NSR systems.

Both nitrite/nitrate and sulfate species were formed on barium when a mixture of NO and SO_2 was introduced to the different samples examined. However, the concentrations of the nitrogen-containing species on the NSR catalyst in this case, were lower than the ones observed in the absence of SO_2, indicating the competitive nature of the NO_x and SO_2 adsorption processes. Our spectroscopic results further indicate that surface sulfate species on barium are slowly converted to bulk barium sulfate, a process which is favored at elevated temperatures. The bulk barium sulfate is very stable under all sets of conditions examined in this study and resists reduction in the presence of propylene. Hence, its formation is consistent with the continuous accumulation (and eventual deactivation of $Pt/BaO/Al_2O_3$ NSR catalysts due to sulfur poisoning) previously reported in the literature.

Acknowledgements

The authors express their gratitude to the Department of Energy (DE_FG02-96ER14666) for the financial support of this work.

References

[1] R.M. Heck, R.J. Farrauto, Catalytic Air Pollution Control, Van Nostrand Reinhold, New York, 1995.

[2] M.D. Amiridis, T. Zhang, R.J. Farrauto, Appl. Catal. B: Environ. 10 (1996) 203.

[3] Y. Traa, B. Burger, J. Weitkamp, Micropor. Mesopor. Mater. 30 (1999) 3.

[4] N. Miyoshi, S. Matsumoto, K. Kasahara, SAE Technical Paper 950809, 1995.

[5] S. Matsumoto, Catal. Today 29 (1996) 43.

[6] N. Takahashi, H. Shinjoh, T. Lijima, T. Suzuki, K. Yamazaki, K. Yokota, H. Suzuki, N. Miyoshi, S. Tateishi, K. Kasahara, Catal. Today 27 (1996) 63.

[7] S. Matsumoto, Y. Ikeda, H. Suzuki, M. Ogai, N. Miyoshi, Appl. Catal. B: Environ. 25 (2000) 115.

[8] S. Matsumoto, Catal. Today 27 (1996) 63.

[9] E. Fridell, M. Skoglundh, B. Westerberg, S.G. Johansson, J. Catal. 183 (1999) 196–209.

[10] H. Mahzoul, J.F. Brilhac, P. Gilot, Appl. Catal. B: Environ. 20 (1999) 47.

[11] L. Lietti, P. Forzatti, I. Nova, E. Tronconi, J. Catal. 204 (2001) 175.

[12] A. Amberntsson, H. Persson, Per. Engström, B. Kasemo, Appl. Catal. B: Environ. 31 (2001) 27.

[13] N. Isabella, L. Castoldi, L. Lietti, E. Tronconi, P. Forzatti, Catal. Today 2747 (2002) 1.

[14] B. Westerberg, E. Fridell, J. Mol. Catal. A: Chem. 165 (2001) 201.

[15] F. Prinetto, G. Ghiotti, I. Nova, L. Lietti, E. Tronconi, P. Forzatti, J. Phys. Chem. B 105 (2001) 105.

[16] H.Y. Huang, R.Q. Long, R.T. Yang, Energy Fuels 15 (2001) 205.

[17] C. Sedlmair, K. Seshan, A. Jentys, J.A. Lercher, J. Catal. 214 (2003) 308.

[18] P.T. Fanson, M.R. Horton, W.N. Delgass, J. Lauterbach, Appl. Catal. B: Environ. 46 (2003) 393.

[19] H. Mahzoul, L. Limousy, J.F. Brihac, P. Gilot, J. Anal. Appl. Pyrol. 56 (2000) 179.

[20] H.Y. Huang, R.Q. Long, R.T. Yang, Appl. Catal. B: Environ. 33 (2001) 127.

[21] C. Sedlmair, K. Seshan, A. Jentys, J.A. Lercher, Catal. Today 75 (2002) 413.

[22] O. Saur, M. Bensitel, A.B.M. Saad, J.C. Lavally, C.P. Tripp, B.A. Morrow, J. Catal. 71 (1991) 319.

[23] M.A. Babaeva, A.A. Tsyganenko, V.N. Filimonov, Kinet. Katal. 25 (1985) 787.

[24] D.K. Captain, M.D. Amiridis, J. Catal. 184 (1999) 377.

[25] A. Amberntsson, M. Skoglundh, M. Jonsson, E. Fridell, Catal. Today 73 (2002) 279.